

## Effects of surface termination on the band gap of ultrabright Si<sub>29</sub> nanoparticles: Experiments and computational models

G. Belomoin,<sup>1</sup> E. Rogozhina,<sup>2</sup> J. Therrien,<sup>1</sup> P. V. Braun,<sup>2</sup> L. Abuhassan,<sup>3</sup> and M. H. Nayfeh<sup>1,\*</sup>  
<sup>1</sup>*Department of Physics, University of Illinois at Urbana-Champaign, 1110 W. Green St., Urbana, Illinois 61801*  
 and <sup>2</sup>*Department of Material Science and Engineering, University of Illinois at Urbana-Champaign, 1110 W. Green St. Urbana, Illinois 61801*  
<sup>3</sup>*Department of Physics, University of Jordan, Amman 11943, Jordan*

L. Wagner and L. Mitas

*Department of Physics, North Carolina State University, 127 Stinson Rd., Raleigh, North Carolina 27695-8202*  
 (Received 8 May 2001; revised manuscript received 30 October 2001; published 10 May 2002)

A Si<sub>29</sub>H<sub>24</sub> particle, with five atoms constituting a tetrahedral core and 24 atoms constituting a H-terminated reconstructed Si surface was recently proposed as a structural prototype of ultrasmall ultrabright particles prepared by electrochemical dispersion from bulk Si. We replace the H termination with a N linkage (in butylamine) and O linkage (in pentane). The emission band for N-termination downshifts by ~0.25 eV from that of H termination, whereas it blueshifts ~0.070 eV for C termination. We use density-functional approaches to calculate the atomic structures and correction from the quantum Monte Carlo method to estimate the highest occupied–lowest unoccupied molecular-orbital band gap. We find a downshift of 0.25 eV for N termination and very little for C termination. These features are discussed in terms of exciton penetration in the capping material.

DOI: 10.1103/PhysRevB.65.193406

PACS number(s): 78.66.Jg, 73.22.–f

Recently, we dispersed bulk Si into monosize ultrasmall nanoparticles of ~1 nm diameter,<sup>1–7</sup> much smaller than what is available today, with high throughput and excellent size definition and control. The particles are extremely active optically in the blue, exceeding the activity of fluorescein, such that single particles are readily detectable.<sup>1</sup> In addition, they exhibit stimulated emission,<sup>2</sup> directed blue beam emission,<sup>3</sup> and harmonic generation.<sup>4</sup> The particle capacitance is ultrasmall, such that single-electron charging and the confinement energy are significantly larger than thermal energies.<sup>5</sup> We synthesize them with H, O, (Ref. 6) or N terminations.<sup>7</sup> Using a density functional approach with generalized-gradient exchange–correlation potentials, configuration interaction, and Monte Carlo approaches, we constructed a structural prototype for 29 atoms (magic number for the Td symmetry). In the prototype, 24 atoms form a network of reconstructed Si-Si species on the surface and five atoms constituting a tetrahedral core.<sup>8</sup>

The optical activity has been analyzed in terms of reconstructed Si-Si network, found only in ultrasmall nanoparticles, on which excited excitons are self-trapped.<sup>9,10</sup> Understanding the chemical interactions and their effect on the optical properties would be very useful for applications in biological imaging and diagnostics.<sup>11–13</sup> In this paper, we examine the structure and optical properties with several termination or linkages: H termination, N linkage (in butylamine) and C linkage (in pentane). The emission and excitation bands are found to down shift by ~0.25 eV for N, but blueshifts by only 0.07 eV for C termination. We calculated<sup>8</sup> the highest occupied–lowest unoccupied molecular orbital (HOMO-LUMO) band gap. The gap with N termination is found to down shift by 0.25 eV from that of H, where as it shifts very little for C termination. These features are discussed in terms of exciton penetration in the capping material.

We disperse Si into nanoparticles by lateral electrochemical etching of (100), oriented, 1–10-Ω cm, *p*-type boron-doped Si wafers in a mixture of hydrogen peroxide (H<sub>2</sub>O<sub>2</sub>), hydrofluoric acid (HF), and methanol. Si acts as the anode, while a platinum wire acts as a cathode. We gradually advance the wafer into the bath to create a large meniscuslike section. The wafer is then immersed in an ultrasound bath, under which the top layer, a weakly interconnected nanostructure network crumbles into ultrasmall particles. H<sub>2</sub>O<sub>2</sub> produces an ideal monohydride stretching phase, and eliminates defects (dihydrides and trihydrides) as well as impurities.<sup>14</sup> Because it oxidizes Si, H<sub>2</sub>O<sub>2</sub> enhances the etching process, resulting in smaller nanostructures. We determined the particle size by high resolution transmission electron microscopy. The measured size of 1 nm was confirmed by auto correlation fluctuation spectroscopy.<sup>5</sup> Previous studies of the precursor solid showed structures of ~1 nm.<sup>15</sup>

N termination follows a recent procedure for terminating porous Si.<sup>16</sup> A chlorobenzene colloid of particles is first saturated with Cl<sub>2</sub>, replacing H with Cl. The dried particles are aminized by butylamine (C<sub>4</sub>H<sub>9</sub>NH<sub>2</sub>) to produce Si-NH(CH<sub>2</sub>)<sub>4</sub>CH<sub>3</sub>.<sup>17</sup> For carbonization,<sup>17</sup> H-terminated (Si-H) Si nanoparticles dispersed in xylene were reacted with 1-pentene (CH<sub>2</sub>C<sub>4</sub>H<sub>8</sub>) to produce Si-CH<sub>2</sub>(CH<sub>2</sub>)<sub>3</sub>CH<sub>3</sub>. To examine the surface termination, we measured the infrared absorption. We measured the transverse optical (TO) infrared vibrations. Figures 1(a)–1(c) give the spectra of the particles on silicon substrates. For H termination [1a], the spectrum shows all H with less than a 10% oxygen signal at 1070 cm<sup>-1</sup>. In the case of N termination [1b], the spectra do not show H bonds. Instead they show a N-H bond at 3300 cm<sup>-1</sup> and butyl groups at 2869, 2881, 2931, and 2966 cm<sup>-1</sup>. The N-H bond indicates a single Si-N linkage. Similarly, in the

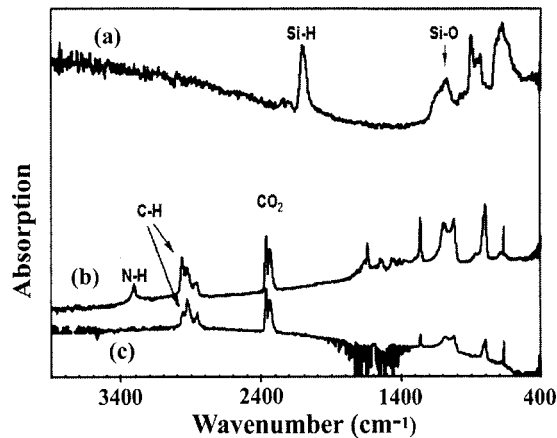


FIG. 1. The FTIR spectra of (a) hydrogenated, (b) aminized, and (c) carbonized particles deposited on silicon substrates. The spectra show the presence of the N-H bond and the methyl groups, in the case of aminization, indicating the Si-N linkage, and it shows the methyl groups in the case of the carbonization, indicating Si-C linkage.

case of carbonization [1c], the spectra show the pentyl groups, indicating an organic coating via Si-C linkage. X-ray photospectroscopy confirms the result.<sup>7</sup> The removal of hydrogen indicates that the functionalization is successful, i.e., Si-H bonds are replaced by Si-N/C linkage.

Figure 2 gives the emission spectrum at 365 nm of the dispersed Si-H, Si-N, and Si-C passivated particles. We used a photon-counting spectrofluorometer with a Xe arc lamp and 4-nm bandpass monochrometers. The emission peak of the hydrogenated particles shifts from 400 to 440 nm upon aminization. In the case of Si-C, the emission band narrows by diminishing the red wing, causing a blueshift of less than 5–10 nm. The emission band of diluted functionalization compounds (by a factor of 20) were measured. Under such dilution the emission from pentene and butylamine (410 nm) is negligible. Emission from the heptane solvent at 355-nm excitation is very weak and broad (2–3 eV), with a peak at 3.2 eV.

We determined the brightness (the product of absorption and quantum efficiency) by fluctuation correlation spectro-

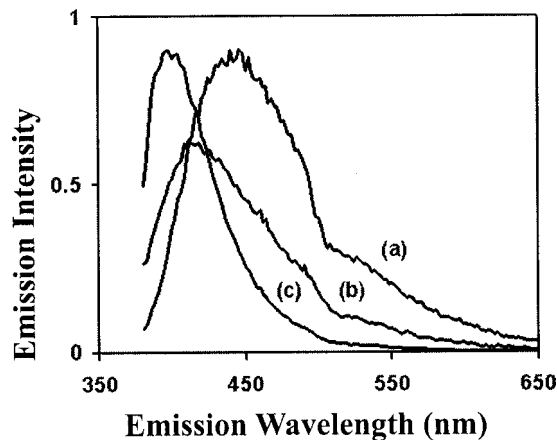


FIG. 2. The emission spectrum at 365 nm of the dispersed Si-H, Si-N, and Si-C terminated particles.

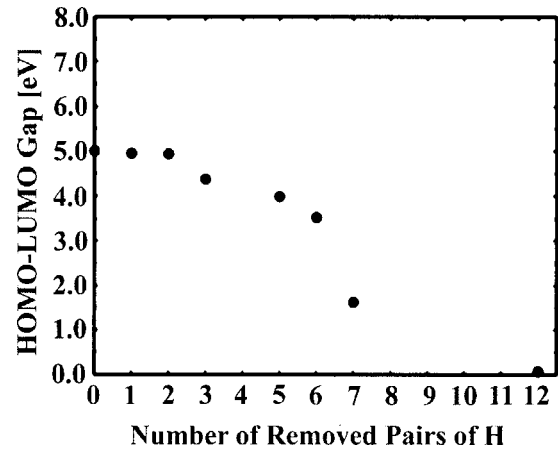


FIG. 3. The calculated band gap of H-terminated particles as a function of the number of H atoms on the particle.

scopy (FCS).<sup>1,7</sup> We used two-photon excitation at 700–900 nm using a mode-locked Ti-sapphire laser (150-fs duration at 80 MHz). At the target, the average power, 20 mW, is focused to a 0.8- $\mu\text{m}$ -diameter spot. The autocorrelation function of the emission  $I: \int I(t+\tau)I(t)^* dt$  of both very diluted particle and standard dye samples are measured. They are fitted to Gaussian diffusion function:  $A [1/(1+8Dt/w^2)] \sqrt{[1/(1+8Dt/z^2)]} + B$ , where  $w$  is the waist of the beam,  $z$  is the depth of the focal volume,  $t$  is in millisecond,  $D$  is the diffusion coefficient,  $B$  is an offset,  $A = 0.076/N$  is the  $t=0$  intercept,  $N$  is the number of particles in the focal volume, and 0.076 is a numerical calibration factor from the standard dye measurement taken under the same beam conditions. We referenced the aminized particle results with those of coumarine. This yields  $w = 400$  nm and  $z = 1.98 \mu\text{m}$ , or a volume of 0.997 picocubic centimeters, and  $N = 1$  particles. This corresponds to a density of  $(3.45\text{--}3.85) \times 10^{12}/\text{cm}^3$ . A similar analysis yields 0.2 coumarine molecules in the focal volume. From the photon-

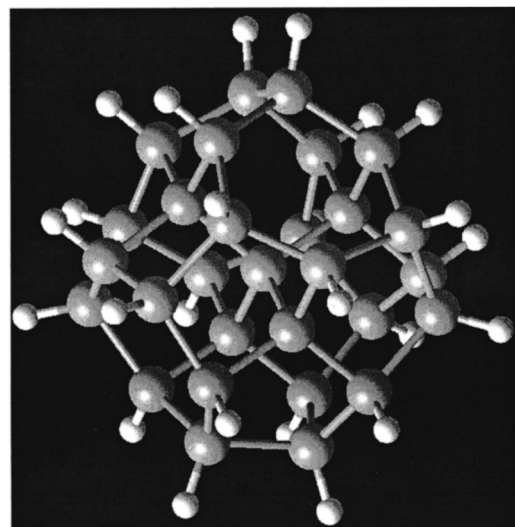


FIG. 4. The  $\text{Si}_{29}\text{H}_{24}$  particle. Five Si atoms (dark sphere) constitute a single tetrahedral core, and 24 Si atoms (dark sphere) constitute a H-terminated (white sphere) reconstructed surface.

counting histograms, we find brightness twofold smaller than coumarine. For the hydrogenated particles, we find brightness two fold to three fold larger than fluorescein.

The computational investigations started with a spherical piece of the bulk Si, which for a size of  $\sim 1$  nm contains 29 atoms (magic number for the Td point group symmetry) and requires 36 H atoms to terminate the unsaturated bonds. The number of H atoms was varied due to reconstruction, as explained below. The geometry optimizations were carried out using density functional generalized gradient approximations with a PW91 functional and 6-31G\* and 6-31G\*\* basis sets. Geometry optimizations and configuration interaction calculations for excited states were carried out in an all-electron framework (no pseudopotentials were employed in this stage). The calculations of the band gap were carried out by using the HUMO-LUMO difference from the PW91 functional corrected by the quantum Monte Carlo (QMC) estimation of the excited state corresponding to the absorption edge and the correction was essentially rigid shift by 0.9(3) eV which corresponded to the 32% percent increase of the band gap as done in our previous calculations<sup>8</sup> based on a combination of methods including the quantum Monte Carlo method.<sup>8,18–21</sup> The QMC calculations employed accurate Hartree-Fock pseudopotentials, which were thoroughly tested in our previous calculation.<sup>22</sup> Due to a loss of elasticity in ultrasmall particles, atoms can move appreciably. Moreover, the presence of H<sub>2</sub>O<sub>2</sub> in the synthesis solution causes a reaction such that an H<sub>2</sub>O<sub>2</sub> molecule may strip two H atoms from adjacent Si sites (forming two water molecules) followed by the movement of the Si atoms to reconstruct. Figure 3 plots the calculated band gap versus the number of H atoms. As the number of H atoms is reduced from 36, the band gap decreases. For less than 24 H atoms, for which each surface Si atom is terminated by a single H atom, it drops sharply, approaching a metallic zero band gap, and the bonding changes from the pure  $sp^3$  tetrahedral diamondlike to the mix with  $sp^2$  type, a configuration common in C that does not exist in bulk Si. In  $sp^2$ , the layers are connected by low-lying  $\pi$  orbitals that are exactly analogous to the conduction bands in metal crystals.  $\pi$  orbitals with delocalized electrons account for the electrical conductivity, for example, in a graphitelike structure. The relaxed configuration, shown in Fig. 4, with five atoms constituting a single tetrahedral core and 24 constituting a H-terminated reconstructed surface (Si<sub>29</sub>H<sub>24</sub>, with six reconstructed dimers) provides the best agreement with our measurements.<sup>8</sup> The

surface is highly wrinkled or puckered system of hexagon and pentagon rings. The prototype gives a diameter of 0.9 nm for the Si core and 10.66 Å including the H termination, and an absorption edge of  $3.5 \pm 0.3$  eV.

For doping by -NH<sub>2</sub> and -CH<sub>3</sub> groups, the positions of the Si atoms are very similar to the pure H terminations. The HUMO-LUMO absorption edge is calculated to be  $3.5 \pm 0.3$ ,  $3.25 \pm 0.3$ , and  $3.55 \pm 0.3$  eV for H, N, and C terminations, respectively. The N termination down shifted the band gap by 0.25 eV relative to the H termination, whereas C termination blueshifted it by a smaller amount. The large  $\pm$  uncertainty is due to a common correction made using Monte Carlo calculations to counter the incomplete treatment of the electron correlation effects,<sup>8</sup> but the relative shifts between the three terminations are more accurate. As expected, the emission spectra correlate with the size of the band gap. It is interesting to consider the valence of the terminating atoms. The N atom has an  $sp^3$  diamondlike hybridization with a bond angle of  $\sim 109.5$  (the tetrahedral angle) to minimize repulsion. Three of the  $sp^3$  orbitals are used to form bonds to Si, H, and  $R=C_4H_9$ , and the fourth orbital holds the lone pair. The N atom, in the Si-N termination, therefore, is of negative valence, i.e., a Lewis base that acts as a hole trap. Trapping the Si hole onto the N site may cause recombination outside the Si material. On the other hand, C is not a Lewis base, i.e., it is not a hole trap; rather it repels the hole, and recombination continues to be on Si sites. The optical properties have been explained in terms of surface reconstructed Si-Si network on which excited excitons are self-trapped.<sup>9,10</sup> The shift due to N termination may be viewed as a softening of the confinement as N allows excitons to combine slightly outside the Si core. The C termination, on the other hand, results in a slight strengthening of the confinement.

We studied the optical properties of Si nanoparticles with H, N and C linkages. The emission downshifts by  $\sim 0.25$  eV for N termination relative to the H termination, but blueshifts by 0.07 eV for C termination. The shifts correlate with shifts in the band gap calculated using the state-of-the-art computational techniques.

The authors acknowledge the State of Illinois Grant ID-CCA No. 00-49106, U.S. NSF Grant No. BES-0118053, U.S. DOE Grant No. DEFG02-ER9645439, NIH Grant No. RR03155, and Motorola. L.M. acknowledges support by NSF Grant No. DMR-0102668.

\*Email address: m-nayfeh@uiuc.edu

<sup>1</sup>O. Akcakir, J. Therrien, G. Belomoin, N. Barry, E. Gratton, and M. Nayfeh, Appl. Phys. Lett. **76**, 1857 (2000); G. Belomoin, J. Therrien, A. Smith, S. Rao, R. Twesten, S. Chaieb, L. Wagner, L. Mitas, and M. Nayfeh, *ibid.* **80**, 841 (2002).

<sup>2</sup>M. Nayfeh, O. Akcakir, J. Therrien, Z. Yamani, N. Barry, W. Yu, and E. Gratton, Appl. Phys. Lett. **75**, 4112 (1999).

<sup>3</sup>M. H. Nayfeh, N. Barry, J. Therrien, O. Akcakir, E. Gratton, and G. Belomoin, Appl. Phys. Lett. **78**, 1131 (2001); M. H. Nayfeh, S. Rao, N. Barry, J. Therrien, G. Belomoin, A. Smith, and S. Chaieb, *ibid.* **80**, 121 (2002).

<sup>4</sup>M. H. Nayfeh, O. Akcakir, G. Belomoin, N. Barry, J. Therrien, and E. Gratton, Appl. Phys. Lett. **77**, 4086 (2000).

<sup>5</sup>J. Therrien, G. Belomoin, and M. H. Nayfeh, Appl. Phys. Lett. **77**, 1668 (2000).

<sup>6</sup>G. Belomoin, J. Therrien, and M. Nayfeh, Appl. Phys. Lett. **77**, 779 (2000); H. Thompson, Z. Yamani, L. AbuHassan, O. Gurdal, and M. H. Nayfeh, *ibid.* **73**, 841 (1998); W. H. Thompson, Z. Yamani, L. H. Abuhassan, J. E. Greene, and M. H. Nayfeh, J. Appl. Phys. **80**, 5415 (1996).

<sup>7</sup>E. Rogozhina, G. Belomoin, J. Therrien, P. Braun, and M. H. Nayfeh, Appl. Phys. Lett. **78**, 3711 (2001).

- <sup>8</sup>L. Mitas, J. Therrien, G. Belomoin, and M. H. Nayfeh, *Appl. Phys. Lett.* **78**, 1918 (2001).
- <sup>9</sup>G. Allan, C. Delerue, and M. Lannoo, *Phys. Rev. Lett.* **76**, 2961 (1996).
- <sup>10</sup>M. Nayfeh, N. Rigakis, and Z. Yamani, *Phys. Rev. B* **56**, 2079 (1997); *MRS Bull.* **486**, 243 (1998).
- <sup>11</sup>See, for example, *Immunoassays*, edited by E. P. Diamandis and T. K. Christopoulos (Academic, New York, 1996); *Protocols for Nucleic Acid Analysis by Nonradioactive Probes*, edited by P. G. Issac (Humana, Totowa, NJ, 1994); *Nonisotropic Probing, Blotting, and Sequencing*, edited by L. J. Kricka (Academic, New York, 1995).
- <sup>12</sup>M. Bruchez, Jr., M. Moronne, P. Gin, S. Weiss, and A. P. Alivisatos, *Science* **281**, 2013 (1998).
- <sup>13</sup>W. C. W. Chan and S. Nie, *Science* **281**, 2016 (1998).
- <sup>14</sup>Zain Yamani, Howard Thompson, Laila AbuHassan, and Munir H. Nayfeh, *Appl. Phys. Lett.* **70**, 3404 (1997); D. Andsager, J. Hilliard, J. M. Hetrick, L. H. AbuHassan, M. Plisch, and M. H. Nayfeh, *J. Appl. Phys.* **74**, 4783 (1993); Z. Yamani, S. Ashhab, A. Nayfeh, and M. H. Nayfeh, *ibid.* **83**, 3929 (1998).
- <sup>15</sup>Z. Yamani, A. Alaql, J. Therrien, O. Nayfeh, and M. Nayfeh, *Appl. Phys. Lett.* **74**, 3483 (1999); Z. Yamani, O. Gurdal, A. Alaql, and M. Nayfeh, *J. Appl. Phys.* **85**, 8050 (1999).
- <sup>16</sup>W. F. Bergerson, J. A. Mulder, R. P. Hsung, and X.-Y. Zhu, *J. Am. Chem. Soc.* **121**, 454 (1999).
- <sup>17</sup>A. Sieval, R. Linke, H. Zuilhof, and E. Studholter, *Adv. Mater.* **12**, 1457 (2000); E. Rogozhina, G. Belomoin, M. H. Nayfeh, and P. V. Braun (unpublished).
- <sup>18</sup>M. J. Frisch *et al.*, GAUSSIAN98, Gaussian, Inc.
- <sup>19</sup>See e.g., E. Artacho and F. Yndurain, *Phys. Rev. Lett.* **62**, 2491 (1989).
- <sup>20</sup>J. B. Foresman, M. Head-Gordon, and J. A. Pople, *J. Phys. Chem.* **96**, 135 (1992).
- <sup>21</sup>L. Mitas, *Comput. Phys. Commun.* **97**, 107 (1996); D. M. Cepereley and L. Mitas, in *Advances in Chemical Physics*, edited by I. Prigogine and S. A. Rice (Wiley, New York 1996), Vol. XCIII, pp. 1–38.
- <sup>22</sup>J. C. Grossman and L. Mitas, *Phys. Rev. Lett.* **74**, 1323 (1995).